Atmos. Chem. Phys. Discuss., 9, 6283–6324, 2009
www.atmos-chem-phys-discuss.net/9/6283/2009/

Atmospheric Chemistry and Physics Discussions

This discussion paper is/has been under review for the journal *Atmospheric Chemistry and Physics (ACP)*. Please refer to the corresponding final paper in *ACP* if available.

Exploring atmospheric boundary layer characteristics in a severe SO_2 episode in the north-eastern Adriatic

M. T. Prtenjak[1], A. Jeričević[2], T. Nitis[3], and Z. B. Klaić[1]

[1]Andrija Mohorovičić Geophysical Institute, Department of Geophysics, Faculty of Science, University of Zagreb, Croatia
[2]Meteorological and Hydrological Service of Croatia, Zagreb, Croatia
[3]Laboratory of Geoinformatics and Environmental Application, Department of Marine Sciences, University of the Aegean, 81100 Mytilene, Greece

Received: 23 December 2008 – Accepted: 19 January 2009 – Published: 9 March 2009

Correspondence to: M. T. Prtenjak (telisman@irb.hr)

Published by Copernicus Publications on behalf of the European Geosciences Union.

Abstract

Stable atmospheric conditions are often connected with the occurrence of high pollutant episodes especially in urban or industrial areas. In this work we investigate a severe pollution SO_2 episode observed on 3–5 February 2002 in a coastal industrial town of Rijeka, Croatia. The episode occurred under anticyclonic high pressure conditions during which a fog, low wind speeds and very high daily associated mean SO_2 concentration of 353.5 $\mu g\,m^{-3}$ were observed. First, the EMEP model was used to evaluate the long-range transport and its contribution to the local SO_2 concentrations. The comparison between the EMEP modelled regional SO_2 concentrations and measured ones in Rijeka showed that the episode was caused predominately by local sources. Furthermore, using three-dimensional, higher-order turbulence closure mesoscale models (WRF and MEMO), the wind regimes and thermo-dynamical structure of the lower troposphere above the greater Rijeka area were examined in detail. The obtained results suggest several factors responsible for elevated SO_2 concentrations. The polluted air is transported towards Rijeka from nearby industrial areas where major pollution sources are located. This transport is associated with strong, ground-based temperature inversion and with a corresponding very low, mixing layer (below 140 m). Light winds or almost calm conditions in Rijeka town were another causative factor of the episode. Also, a vertical circulation cell formed between the mainland and a nearby island, causing the air subsidence and stability increase in the lowermost layer south of Rijeka.

1 Introduction

Facing the Adriatic Sea and surrounded by mountains (Fig. 1), Rijeka is a coastal industrial town situated in a region of very complex wind regimes (e.g. Klaić et al., 2003; Nitis et al., 2005; Prtenjak et al., 2006; Prtenjak and Grisogono, 2007; Prtenjak et al., 2008a). In the Greater Rijeka Area (GRA), southeast of the city of Rijeka, some of the

ACPD

9, 6283–6324, 2009

major individual sources of SO_2 in Croatia are found, such as an oil refinery and a thermal power plant. According to estimates from the Ministry of Environmental Protection, Physical Planning and Construction of the Republic of Croatia (http://www.mzopu.hr, data for 2002) the two sources emit about 20% of the total national emissions of SO_2, where 8933 and 4909 tones of SO_2 correspond to the oil refinery and thermo-power plant, respectively. In addition, compared to other regions along the eastern Adriatic coast, the GRA – together with the Istria peninsula – is more exposed to the long-range transport of pollutants from western Europe (e.g. Klaić, 1996, 2003; Klaić and Beširević, 1998).

In terms of air quality protection, knowledge of the basic characteristics of the wind and thermodynamic conditions is essential, especially in cases of severe air pollution episodes (Skouloudis et al., 2009). An air pollution episode is defined as an event in which concentrations of air pollutants increase substantially above the national standard limit (Fisher et al., 2005). Pollution episodes can occur due to various causes, such as, increased pollutant emissions, topographical (e.g. Brulfert et al., 2005) and/or thermal forcing (e.g. Robinsohn et al., 1992; Evtyugina et al., 2006; Drobinski et al., 2007; Levy et al., 2008), favourable weather conditions and season or chemical characteristics of the atmosphere. Results of many studies (e.g. Robinsohn et al., 1992; Soler et al., 2004; Pohjola et al., 2004; Fisher et al., 2005; Tayanc and Bercin, 2007) showed that severe air pollution episodes around the world are very often associated with high-pressure conditions, weak winds and/or strong low-level temperature inversion and poor vertical mixing (e.g. Natale et al., 1999). In some cases occurrence of high level SO_2 episodes have been caused by long range transport (e.g., Steenkist, 1988; De Leeuw and Leyssius, 1989).

Recently, a human health risk event occurred in Rijeka during 3 to 5 February 2002, where a daily mean concentration of SO_2 reached the high value of 353.5 $\mu g\,m^{-3}$, which is about 10 times the average daily value in February and double the limit value of 125 $\mu g\,m^{-3}$ (http://www.zzjzpgz.hr/zrak/index.php). Therefore, on 4 February, the local authorities warned the Rijeka inhabitants to remain indoors. Potential sources for

ACPD
9, 6283–6324, 2009

the high SO_2 levels were the oil refinery and thermal power plant, but both claimed that during the episode their emissions were at normal levels.

A previous study of the same episode (Jeričević et al., 2004) suggested fumigation due to high-pressure conditions and consequent weak circulation as the cause. However, this study was based on simulations provided by the operational hydrostatic weather forecast model ALADIN (*Aire Limitée Adaptation dynamique Développement InterNational*) (Geleyn et al., 1992) at a horizontal resolution of 8 km, and accordingly smoothed terrain topography. Thus, it did not offer a detailed insight in the fine-scale (~1 km) lower-tropospheric phenomena, characterizing this particular event, which, we believe, we have succeeded in doing in the present study. The more so, the weak wind speeds and calms are frequent for Rijeka (see e.g. Prtenjak and Grisogono, 2007), and they are not always accompanied by elevated pollutant concentrations. Thus, they are not necessarily indicators of pollution episodes. Another novelty of this study, compared to the investigation of Jeričević et al. (2004), is an assessment of the relative contribution of distant pollution sources in the occurrence of the observed elevated SO_2 concentrations. For this purpose, we applied the Unified European Monitoring and Evaluation Programme (EMEP) model (Simpson et al., 2003) that simulates atmospheric transport and deposition of pollutants at regional and synoptic scale. This episode is the subject of study within the EMEP4HR project. A companion paper (Jeričević et al., 2009) will address chemical transport modelling with a fine-scale version of the EMEP model. In this paper we briefly illustrate the episode and results from the standard (50 km) EMEP model, but concentrate on the meteorological situation, illustrating the capabilities of two mesoscale NWP models, and in particular WRF.

2 Study area and data

The GRA is located in the western part of Croatia (Fig. 1a) and is characterized by a complex topography. It is a mountainous area open to the sea towards the south, where several islands are located, with Cres and Krk being the largest (Fig. 1b). The

Rijeka urban area faces the Kvarner Bay. The Kvarner Bay is surrounded with rather high mountains: Risnjak (more than 1250 m high), Velika Kapela (1534 m) and Velebit (1758 m) mountains with steep slopes. Westward from Rijeka, the terrain rises very abruptly along the coastline (Učka and Ćićarija mountains, 1401 m, and 1272 m, respectively), forming a physical boundary between the Istria peninsula and the Kvarner Bay. A more gradual rise of the terrain is found north-west of the Rijeka urban area, with an elevation of less than 500 m a.s.l., where a roughly triangular valley extends towards the Gulf of Trieste (GT in Fig. 1), which is near the north-western boundary of the study area.

Meteorological data from main and ordinary meteorological stations in the north-eastern Adriatic region were used in order to investigate the temporal variations of the wind field. The details on measuring sites are listed in Table 1, and their locations are shown in Fig. 1.

Meteorological charts over Europe for the period of study show a high pressure field over the central and south-eastern part of Europe. Here we show only one snapshot of the surface conditions over Europe (Fig. 2). Over the north-eastern Adriatic coast these were accompanied by weak pressure gradients with consequent weak surface winds, and stagnant conditions with fog and low stratified cloudiness. On 5 February, the high pressure field started to weaken, indicating the change of synoptic forcing due to the Genoa Cyclone that approached the Kvarner Bay (not shown). Additionally, the radio-sounding performed in Udine (coarse domain; Fig. 1a) revealed a high static stability ranging from 5.6 K km^{-1} on 2 February to 5.2 K km^{-1} on 5 February. During the entire period under study, the winds in the lowermost 2 km in Udine were mostly less than 4 m s^{-1}, and varied from south-westerly to westerly.

The hourly and daily measured averaged SO_2 concentrations observed in Rijeka_3B (Fig. 1c) from 1 to 6 February 2002 are shown in Fig. 3. The SO_2 concentrations start to increase on 3 February (from 09:00 local time, LT) and continue to grow the next day reaching the highest hourly concentrations at 10:00 LT on 5 February (around 600 µg m^{-3}). As of 5 February 12:00 LT concentrations started to decrease. Thus, after

13:00 LT they are below 150 $\mu g\,m^{-3}$. This pollutant concentration decrease coincided with the change of large-scale synoptic conditions. The highest daily mean concentration occurred on 4 February reaching a value of 353.5 $\mu g\,m^{-3}$ which is about 10 times higher than the average.

3 The EMEP model

Here, the daily regional SO_2 concentrations have been calculated with the Unified EMEP model (http://www.emep.int/) that was developed at the Norwegian Meteorological Institute (MET. NO.) and is fully documented in e.g. Simpson et al. (2003) and Fagerli et al. (2004). The EMEP model is a multi-layer dispersion model which simulates the long-range transport and deposition of air pollution i.e. acidifying and eutrophying compounds, photo-oxidants and particulate matter, providing critical levels of pollutant concentrations at a daily scale for regulatory purposes. The EMEP domain covers Europe and the Atlantic Ocean, with a horizontal resolution of 50 km and with 20 terrain-following layers in vertical up to 100 hPa. The meteorological input is obtained every 3 h, by the PARallel Limited Area Model with Polar Stereographic map projection (PARLAM-PS), a version for EMEP of the HIgh Resolution Limited Area Model (HIRLAM) a numerical weather prediction model. Horizontal advection is based upon the scheme of Bott (1989a, 1989b) and the vertical diffusion scheme is based on the O'Brien function (1970). A pre-processing program interpolates the data field of interest to the EMEP providing monthly averaged boundary conditions. The necessary anthropogenic emissions input for SO_2, NO_x, CO, NH_3, Nonmethane Volatile Organic Compounds (NMVOC) and particulates are specified according to the annual national emissions reported per sector and grid, giving the model output as daily means.

Currently, considerable scientific effort is being invested in the further development of the EMEP modelling system in order to make it applicable at finer resolutions (i.e. national scales and finer time scales). Thus, there are two such ongoing joint projects: one for the UK domain (EMEP4UK, Vieno et al., 2008, 2009), and the other for Croatia

(EMEP4HR, Jeričević et al., 2007).

In addition, air trajectories were calculated by tracking an air parcel every 2 h for 96 h backwards in time for 4 different starting terms i.e. 00:00 UTC, 06:00 UTC, 12:00 UTC and 18:00 UTC. For each single term, two-dimensional trajectories are defined by a total of 49 position points (including the arrival point). The trajectories calculations were based on meteorological data from the model PARLAMPS in the EMEP grid developed at the MET. NO. Modelled wind fields at 925 hPa have been used for the calculations, as well as the precipitation fields. Assimilated precipitation fields based on actual observations have been used in the calculations.

4 Mesoscale models

Smaller-scale meteorological conditions were simulated by two mesoscale models. The first model was the mesoscale Weather Research and Forecasting model (version 2.2) (WRF, http://www.wrf-model.org/index.php; Skamarock et al., 2007). WRF was developed at the National Centre for the Atmospheric Research, operated by the University Corporation for Atmospheric Research. WRF (http://www.wrf-model.org/index.php) represents the state-of-the-art atmospheric simulation system used in a variety of areas (Michalakes et al., 2004) including storm prediction and research (e.g. Kain et al., 2006), air-quality modelling (e.g. Jimenez-Guerrero et al., 2008), wildfire, hurricane (e.g. Trenberth et al., 2007), tropical storm prediction and regional climate and weather prediction (e.g. Skamarock and Klemp, 2008). The WRF model consists of fully compressible non-hydrostatic equations on a staggered Arakawa C grid. Thus, the wind components u, v, and w are recorded at the respective cell interfaces and all other variables, as volumetric cells, carry averages at the cell centre. Its vertical coordinate is a terrain-following hydrostatic pressure coordinate. Here, the model uses the Runge-Kutta 3rd order time integration scheme and 5th order advection schemes in horizontal direction and the 3rd order in vertical ones. A time-split small step for acoustic and gravity-wave modes is utilized. The dynamics conserve scalar variables.

ACPD
9, 6283–6324, 2009

In this study a two-way nested option was used, where a horizontal step of the coarse domain was 9-km (on the Lambert conformal projection). The coarse domain of 648 km×648 km covers the major portion of the Adriatic Sea area (frame A in Fig. 1a). The medium domain of 318 km×318 km with a horizontal resolution of 3 km covers the Kvarner Bay (frame B in Fig. 1a). The fine-grid domain corresponds to an area of 130 km×124 km and 1 km horizontal resolution (frame C in Fig. 1a), and it captures the GRA. Sixty-five terrain-following coordinate levels were used with the lowest level at about 25 m. The spacing between levels gradually increases from 50 m at the bottom to 300 m in the middle and upper troposphere, and finally to 400 m toward the top that was set at 20 km. The WRF dynamical and physical options used for all three domains are: the ARW dynamical core; the Mellor-Yamada-Janjic (MYJ) scheme for the planetary boundary layer (PBL); the rapid radiative transfer model for the long-wave radiation and the Dudhia scheme for shortwave radiation; the single-moment 3-class microphysics' scheme with ice and snow processes; the Eta surface layer scheme based on the Monin-Obukhov theory and the five-layer thermal diffusion scheme for soil temperature. For the coarse 9-km domain the Betts-Miller-Janjic cumulus parameterization is employed, however without parameterization in the inner domains. Initialization and boundary conditions were taken from the European Centre for Medium-Range Weather Forecasts (ECMWF) Reanalysis fields. The ECMWF data were available at a 0.25-degree resolution (~25 km resolution) at the standard pressure levels every 6 h. Simulation was performed from 12:00 UTC of 31 January to the 00:00 UTC of 6 February. During the studied period, the observed sea surface temperatures were almost constant in time and space (~9.5°C). Therefore, the WRF version with the time-constant sea surface temperature was employed.

The second mesoscale model used was the MEsoscale MOdel (MEMO) version 6, which belongs to the European Zooming Model system for simulations of wind flow and pollutant transport and transformation (Moussiopoulos, 1995). The model has been previously validated against extensive data sets such as for Athens (Kunz and Moussiopoulos, 1995), Barcelona (Soriano et al., 2001), Zagreb (Klaić and Nitis, 2001–2002;

ACPD
9, 6283–6324, 2009

Klaić et al., 2002; Nitis et al., 2009) or Rijeka (Nitis et al., 2005; Prtenjak et al., 2006). A one-way nested system based on the expanded radiation boundary conditions was applied, in order to account for all relevant topographic influences on the flow field. Two domains were used: a coarse grid domain of 300 km×300 km and 3 km horizontal resolution (similar to B in the WRF simulation) and a fine grid domain of 100 km×100 km and a horizontal resolution of 1 km (similar to the grid C in WRF). In the vertical, 25 layers were assumed with the model top set to 6 km, in order to incorporate the larger-scale forcing better. Meteorological input information, consisting of vertical profiles of wind speed, wind direction and temperature, was obtained by the Udine and Zagreb radio-sounding stations. A very detailed orography data set (with a horizontal grid of approximately 90 m) for the study area was derived from the Shuttle Radar Topography Mission (SRTM, Farr et al., 2007) database and the land use data set originated from the Corine land cover 2000 (CLC 2000) database which includes 44 land cover types with a horizontal resolution of about 100 m. In MEMO6, the original 44 land use types are reclassified into 11 more general ones.

5 Results

5.1 The EMEP model results

According to Fig. 3, the observed daily concentration of SO_2 started to increase considerably on 3 February 2002 (an approximate increase of 300%). The first step was to evaluate a possible contribution of the long-range SO_2 transport which is provided by the EMEP model. The EMEP modelled concentrations exhibit increased values during the episode, especially at its beginning (on 3 February, Fig. 3). The increase in the EMEP concentrations means that the regional meteorological conditions favour the long-range SO_2 transport concentrations in Rijeka. Trajectories (Fig. 4) exhibited that approximately 2 days before the occurrence of the episode, transboundary polluted air was crossing above known main regional emission sources of SO_2: in Hun-

gary, Bulgaria and central Bosnia, as well as central Italy (not shown). Parcel positions were very close, especially for the last 24 h, meaning that modelled wind speeds were low ($<5\,m\,s^{-1}$) and stagnant conditions were present over the larger regional area, connected with the formation of a high pressure system. Different starting times of trajectories revealed westward shift. Still, the EMEP modelled values comprised only up to about of 2% of the observed concentrations, confirming that the majority of the observed high SO_2 concentrations arise from local emission sources.

5.2 The mesoscale models performances

In order to validate the WRF simulation results, we compared them to the available surface observations furnished by the main meteorological stations in the fine-grid domain (shown in Fig. 1b). Table 2 presents only one statistic index, the index of agreement, *d*, (e.g. Willmott, 1982) among others calculated statistic indices (not shown) (Nitis et al., 2007). The shown parameter in Table 2 reflects the degree to which measurements are accurately estimated by the model. The calculations were made for wind speed, wind direction and temperature at four stations with 24 h measurements. During 2–5 February, the *d*-index, for all the aforementioned variables showed reasonable model performance, although somewhat poorer agreement was obtained for the wind speed in the 3A (Rijeka) site (Table 2 and Fig. 5a). At this site, Fig. 5b, wind direction is reproduced reasonably well. The measuring site is sheltered for north-easterly flows and the wind speed overestimation for the north-easterly directions has already been observed there (Klaić et al., 2003). Due to low wind speeds, the measured wind directions are highly variable, while the modelled ones are more organized into local flows. Such recorded low wind speeds ($<2\,m\,s^{-1}$) are generally difficult to model (e.g. Mahrt and Vickers, 2006; Mahrt, 2007). The smoothing of the model terrain at the 1 km resolution, and the parameterization of turbulent fluxes during the night in the stable boundary layer according to the Monin-Obukhov theory (e.g. Grisogono et al., 2007; Baklanov and Grisogono, 2007) are the most probable causes. The air temperature at 2 m in Rijeka is generally overestimated (Fig. 5c). Still the agreement is accept-

able (Table 2) especially in respect to the local observed fog formation, weak winds and almost equal sea and air surface temperatures during the studied period. Finally, knowing the overwhelmingly complex terrain, finite resolution of the model and its parameterizations, the overall correspondence between measurements and the WRF model is satisfactory.

The same statistical index was calculated for MEMO, as well. In general, results obtained by the WRF were somewhat better compared to the MEMO results (not shown) and therefore, we will focus on the WRF results. However, respecting models deviations from measurements, some basic meteorological characteristics were simulated by both models (Prtenjak et al., 2008b).

5.3 The modelled WRF horizontal fields

On 2 February sunny conditions were observed in the GRA and the maximum air temperature there was higher than the sea surface temperature by 10°C. Thus, a growth of the mixed layer is expected, which is potentially accompanied by the mixing down of elevated pollutants present in the residual layer from the previous day (Stull, 1988). Jeričević et al. (2004) assumed that the observed SO_2 concentration growth on 3 February was due to pollutant entrainment into the boundary layer from the previous day. Still, their model results did not allow final conclusion. Since the maximum concentration occurred on the 4 February, we mostly focus on the lower-tropospheric conditions during the pollution episode, from 2 to 4 February 2002. Figure 6 shows the simulated 10-m wind field on 2 February 2002 at 14:00 LT. Both measurements and simulation results show prevailing north-westerly winds over the western part of the Istria peninsula (Fig. 6a, b). The simulated wind field suggests an advection of the marine moist air towards land, which explains the observed fog above the western Istrian coast.

However, the WRF model slightly overestimated the measured air surface temperature over west Istria (not shown here). Compared to the west coast, above the central part of the Istria peninsula, both measured and simulated (Fig. 6c) maximum daily tem-

ACPD
9, 6283–6324, 2009

peratures are higher. Such a temperature pattern extends towards the GRA, where the model values are slightly lower than the measured ones. Regarding the wind field, (Fig. 6a, b), blocking is established at the windward side of mountains Ćićarija, Učka and Risnjak. Owing to the upstream blocking inside a roughly triangular valley stretching toward the Gulf of Trieste, the winds are weak. Between the island of Cres and Istria the wind veers toward south-westerly. Over the western, lee sides of the Učka mountain, the island of Cres and over a large portion of the Velika Kapela and Velebit mountains, the downslope flow accelerated flow is found due to radiative cooling of the mountain slopes. Above Rijeka, the north-eastern flow meets the south-westerly winds blowing over the Rijeka Bay resulting in an onshore flow above the coastline. Although light, these winds ventilated the GRA, and thus, daily SO_2 concentration was relatively low (Fig. 3). Between the islands of Krk and Cres, as well as inside the Velebit channel (VC in Fig. 1), the northerly channelled flows establish.

During the evening hours of 2 February (21:00 LT, Fig. 7), the airflow pattern at the western coast of Istria is similar to the daytime one (14:00 LT, Fig. 6). The downstream flow still occurs at the western slopes of the high mountains (Fig. 7b). However, above the Rijeka Bay and the island of Krk, the wind regime started to change. As of 18:00 LT (not shown here) the anti-clockwise mesoscale eddy, associated with katabatic winds channelled within the pass between Risnjak and Velika Kapela, extends over the greater Rijeka area. A similar wind pattern, which is due to topography, has already been suggested by Prtenjak et al. (2006) for the night time stable conditions during summer. Above the island of Krk, especially over its eastern part (Fig. 7b), south-easterly winds blow. Thus, they transport the air from the northern Krk, where the petrochemical plant and the oil terminal are located (point 2, Fig. 1c) towards the Rijeka town. Further, the established mesoscale vortex transports the air from the industrial zone of Rijeka (point 1, Fig. 1c) towards the town (Fig. 7). The transport of air above the areas with major pollution sources is accompanied by a gradual increase of atmospheric stability due to the nighttime cooling (not shown). A very similar wind field, especially concerning the south-easterly winds connected with the mesoscale vortex,

ACPD
9, 6283–6324, 2009

was obtained by the MEMO model, as well (not shown here).

On 3 February, measurements show weak winds (lower than 4.5 m s^{-1}) over Rijeka throughout the day. Over the western part of the Istria peninsula, easterly winds blow in the morning; south-easterly ones around noon, and eventually in the evening they vary randomly from northerly to easterly ones (not shown). In the central part of Istria wind directions are almost "frozen" in time, while magnitude slightly varies. Figure 9 depicts the observed and modelled winds for 3 February at 14:00 LT. The modelled winds are very weak (up to about 4 m s^{-1}) over the entire coastal zone. Further, the cyclonic eddy is almost continuously present above the Rijeka Bay (Fig. 8b). Bearing in mind the low wind speeds, the agreement between the measured and simulated wind vectors is satisfactory, with discrepancies at the southern tip of Istria being somewhat larger. According to the modelled wind fields, over the western coast of Istria, the westerly flow continues bringing the moist marine air over land. This further supports the persistence of fog, which according to measurements was reported for all coastal sites. Similarly, the previous evening, the modelled wind field exhibits a south-easterly flow which transports the air from local emission sources towards Rijeka town (Fig. 8b). These results were obtained by MEMO as well (Prtenjak et al., 2008b). It is important to note that the airflow pattern over the greater Rijeka Bay area, in Fig. 8b, is almost stationary throughout the 3 February. On the other hand, in the mountain pass between Ćićarija and Risnjak, the airflow conditions change and winds turn to south-easterly ones. Modelled temperatures are generally higher than measured ones (not shown). Further, the modelled temperature field pattern is similar to the pattern of the previous day, although the values are somewhat lower. In time, the atmosphere becomes more stable due to continuous nighttime radiative cooling of the land. The stable stratification suppresses the vertical mixing inside the boundary layer, which results in very weak nighttime winds especially above the Kvarner Bay. Over the major part of the Istrian peninsula, the modelled airflow is eastern, which agrees well with the measurements. The synoptic forcing is weak. Hence, both the complex topography and the stable stratification strongly influence the local winds.

During the night and morning hours of 4 February, stagnant surface wind conditions persisted almost everywhere in the coastal area. At 07:00 LT (Fig. 9), over the major portion of Istria weak easterly winds are present and downslope flows are established over the eastern slopes of the Ćićarija, Učka, V. Kapela and Velebit mountains. North of Rijeka, the drainage winds of cold surface air are blocked upon reaching a relatively warmer sea (Fig. 9b and c). The existence of the weak south-easterly winds above Omišalj that veer toward easterly winds above Rijeka can still be noted until 13:00 LT (not shown) in the about 400 m deep surface layer. These fairly weak winds likely support the air-mass stagnation and the pollutant accumulation in the lower atmospheric layer above Rijeka, thus resulting in the highest daily measured SO_2 concentration. Stagnant winds and overall weak synoptic forcing favour fog formation and short-lasting drizzle, which were reported for the coastal sites. Fog and drizzle are generally associated with strong static stability, which was found in this particular region (see Figs. 13 and 15). According to model results, as of 4 February at 14:00 LT atmospheric conditions gradually changed and a north-westerly flow of moderate intensity started to establish in the GRA (Fig. 10). Therefore, there were no more conditions supporting the transport of air from the industrial areas towards the Rijeka town. Specifically, the wind became channelled by the island of Cres and Istria. Thus, a very weak clockwise eddy forms, which transported air towards the island of Krk, and cancelled any earlier anti-clockwise vortex inside the Rijeka Bay. The same is confirmed by measurements (Fig. 10a and b). Generally, wind speeds remained lower than 5 m s^{-1} until the 21:00 LT. The airflow strengthened afterwards, especially over the southern tip of the Istria peninsula.

The afternoon wind distribution of the previous day mostly retains until 08:00 LT of 5 February (not shown). Around noon, the CW eddy within the Rijeka Bay starts to diminish and south-easterly winds form through the Velebit channel. In the afternoon prevailing southerly winds dominate in the whole studied area (Fig. 11) changing the atmospheric conditions. In the GRA, winds fortify until the end of the day. This is in agreement with the decrease in SO_2 concentrations on 5 February.

ACPD
9, 6283–6324, 2009

5.4 The modelled WRF vertical cross-sections

Modelled vertical cross-sections of potential temperature and wind vectors at 09:00 LT and 18:00 LT on 3 February are presented in Fig. 12. Here, the analysis is concentrated on the GRA regarding static stability and wind field. At 09:00 LT (Fig. 12a) a different boundary layer development can be noted above the coast compared to adjacent foothills. The coastal shallow (≈200 m deep) stable layer is under the influence of the incoming south-easterly flow (Fig. 12b). A somewhat less stable layer is formed north-eastward (region above 27 km$<x<$34 km in Fig. 12a) which is characterized by local mixing, with a subsidence above the sea and an upslope flow along the foothill above Rijeka. During the day, the difference between the ground-based layers above the Rijeka and adjacent foothills disappears and static stability increases (Fig. 12c, d). Under such circumstances, air ventilation is poor and winds are week. However, the southern airflow component persists further supporting the transport of air from industrial regions towards Rijeka. Further, it is interesting to notice the circulation cell, approximately 350 m deep, which is found between the mainland and the island of Cres above the lowermost approximately 100 m (bottom panel, right). This circulation cell in the vertical plain acts as a lid, which prevents the pollutants in the lowermost ground-based layer to dilute. During the night time, due to persistent subsidence and radiative cooling, the static stability increases (not shown), which further favours the pollutant accumulation in the lowermost atmospheric layers. Such pollution episodes, due to temperature inversions resulting in the stagnant air, have already been observed elsewhere (e.g. Fisher et al., 2005).

As stated above, during the first part of 4 February, the weak anticlockwise surface wind eddy still exists above the major portion of the Rijeka Bay. Thus, the transport of air from both the northern part of the island of Krk and the industrial zone southeast of town, continues, although south-easterly winds are rather weak. Simultaneously, apart from confirming the existence of south-easterly winds, the vertical fields (Fig. 13, for 08:00 LT) reveal further increase of the static stability over Rijeka, which is accom-

ACPD
9, 6283–6324, 2009

panied with the subsidence. Thus, the maximum daily mean SO_2, which is recorded on 4 February, can be attributed to the shallow and very stable ground-based layer with generally weak, predominantly south-eastern, winds found in the first 200 m of the troposphere. In the afternoon hours (Fig. 13c, d), the wind direction changes, and subsidence over the Rijeka region, in the elevated layer extending from about 200 m to 1 km, increases. Consequently, the static stability within this layer also increases and further prevents pollutant dilution within the layer below (i.e. within the lowermost layer). In addition, winds in the lowermost layer remain weak. Accordingly, the SO_2 concentrations (Fig. 3) remain high until midday of 5 February.

The vertical fields on 5 February show once more the daytime south-easterly winds above the major portion of the GRA (Fig. 14). The transport of air from both, the northern part of the island of Krk and the industrial zone southeast of the town is established again. However, the winds become stronger and static stability decreases over Rijeka (especially during the evening hours) which agrees with the decreasing in of the SO_2 concentrations (Fig. 3).

5.5 The modelled WRF potential temperature profiles and boundary layer heights

The evolution of vertical profiles of potential temperature from 2 to 5 February above Rijeka is shown in Fig. 15. Ground-based temperature inversion, which is present on 3 February at 09:00 LT in the first 200 m, strengthens in time. Above the lowermost layer, the most stable one, another stable layer of somewhat weaker static stability exists. In time, its stability also increases up to the 4 February reaching the maximum stability. Conditions on 5 February are characterised by a decrease of SO_2 concentrations, lower static stability in the morning and relatively high mixing in the evening.

According to the model setup (MYJ scheme), the PBL is described by the one-dimensional prognostic turbulent kinetic energy scheme with local vertical mixing. Therefore, the PBL top depends on the TKE as well as the buoyancy and shear of the driving flow. In the stable range the upper limit of the PBL is deduced from the requirement that the ratio of the variance of the vertical velocity deviation and the

TKE cannot be smaller than that corresponding to the regime of vanishing turbulence (http://www.wrf-model.org/index.php).

The daily course of the PBL height above Rijeka during the polluted episode is shown in Fig. 16. According to the modelled PBL height of Rijeka, the daily maximum on 2 February were around 900 m. Higher air temperatures above Rijeka are connected to the higher boundary layer (see also Fig. 15) that can result by the pollutant entrainment into the boundary layer of the residual layer from the previous day. The next day, following the temperature daily cycle, maxima PBL heights were less than 400 m. On 4 February, during the maximum daily SO_2 concentrations as well as the maximum static stability (Fig. 15), the daily PBL heights were below 140 m. For the same period, Jeričević et al. (2004) obtained more periodically and much higher mixing heights. They evaluated them from the ALADIN model (8 km resolution) with the bulk Richardson number method for Rijeka. The conclusion was that the ALADIN model unrealistically overpredicted 2-m air temperature for days with fog, giving mixing height maxima around 400 m. Here, the 2-m temperatures, as well as the PBL heights, are simulated more realistically (Figs. 5c, 16). It is interesting to note that the increase in the PBL heights is connected to the small gap in the hourly SO_2 concentrations on 3 February from 11:00 LT–15:00 LT (compare Figs. 3 and 16). Likewise, on 5 February, the increse of the PBL height (Fig. 16) and the decrease of the static stability (Fig. 15) results in the hourly SO_2 concentrations decrease after 11:00 LT (Fig. 3).

6 Conclusions

We examined the relationships between modelled mesoscale wind and temperature fields and high SO_2 concentrations recorded on 3–5 February 2002 in the coastal town of Rijeka. Although the hourly concentrations gradually grew toward the highest value on 5 February, the maximum daily SO_2 concentration occurred on 4 February causing very dangerous health conditions for the inhabitants of Rijeka. The episode took place during anticyclonic high pressure conditions. During the episode, in Rijeka, maximum

air temperatures were mostly lower than sea surface temperatures with low daily air temperature amplitude (around 3°C). Under such circumstances fog developed along the coast and wind speeds were low.

For the investigated episode, the EMEP model results suggested higher SO_2 concentrations compared to usually modelled concentrations due to distant pollution sources. This means that meteorological conditions were favourable for both local and long-range transport in corresponding stable conditions. The horizontal daily surface SO_2 distribution and trajectories exhibited a long-range transport of polluted air from Bulgaria, Bosnia and Italy. However, the long-range transport of SO_2, estimated by the EMEP model, shows relatively small contribution to the overall recorded SO_2 concentrations in Rijeka.

The mesoscale model results demonstrated a successful multi-day simulation in the GRA and reasonable agreement with the available observations. Here two mesoscale models were used; the WRF and the MEMO, with emphasis on the WRF model which gave better simulated results. The WRF model results suggest several factors which can be responsible for the occurrence of the severe pollution episode. These are as follows.

- Transport of air from regions with major pollution sources towards Rijeka by south-easterly winds. These surface winds are often connected to the anti-clockwise eddy inside the Rijeka Bay, which maintains the transport of polluted air above the island of Krk, especially over its eastern part where the petrochemical plant and the oil terminal are located.

- The abovementioned transport of air from the areas with major pollution sources is accompanied by a gradual increase of atmospheric stability during the episode. The maximum static stability occurred on 4 February limiting the dispersion of pollutants in the very low (within 140 m) mixing layer. The mixing layers were associated by the formation of a strong ground-based radiation inversion in the GRA.

ACPD
9, 6283–6324, 2009

– The surface wind field shows the stagnation region of airflow upstream of Rijeka which is favourable of pollutant accumulation (especially during 4 February).

– The air subsidence in the lowermost layer south of Rijeka, further facilitates pollutant accumulation. The subsidence is a result of the circulation cell, approximately 500 m deep, which is found between the mainland and the island of Cres above the lowermost approximately 100 m (on 3 February). This circulation cell in the vertical plain acts as a lid, which prevents the pollutants in the ground-based layer to dilute. During the next day, the drainage flow occurred above the circulation cell that existed in the first 200 m where the wind profile exhibited calm or lower wind less than 1 m s^{-1}. The drainage flow was related to the increase of wind speed enhancing static stability above Rijeka.

Finally, it can be summarized that that the local meteorological conditions were very favourable for the formation of a severe pollution episode. Still, there is an open question in the case that local emissions were not higher than usual, as claimed by local industrial plant administrations.

Acknowledgements. We are very grateful to Teaching Institute for Public Health, Rijeka for SO_2 data and Ana Alebić-Juretić (from the same Institute) for available comments. Also, we are indebted to the Meteorological and Hydrological Service of the Republic of Croatia and the Meteorological Department of the Croatian Air Traffic Control at Zagreb Airport for providing the meteorological data. This work has been supported by the Ministry of Science, Educational and Sport (grants No. 119-1193086-1323 and No. 119-1193086-1311) and EMEP4HR project number 175183/S30 provided by the Research Council of Norway.

References

Baklanov, A. and Grisogono, B.: Amospheric Boundary Layers: Nature, Theory and Applications to Environmental Modeling and Security, 241 pp., Springer, 2007.

Bott, A.: A positive definite advection scheme obtained by non-linear renoramlization of the advection fluxes, Mon. Weather Rev., 117, 1006–1015, 1989a.

Bott, A.: A positive definite advection scheme obtained by nonlinear renormalization of the advective fluxes – reply, Mon. Weather Rev., 117, 2633–2636, 1989b.
Brulfert, G., Chemel, C., Chaxel, E., and Chollet, J. P.: Modelling photochemistry in alpine valleys, Atmos. Chem. Phys. 5, 2341–2355, 2005.
De Leeuw, F. A. A. M. and Leyssius, H. J. V.: Long-range transport modelling of air pollution episodes, Environ. Health Persp., 79, 53–59, 1989.
Drobinski, P., Said, F., Arteta, J., Augustin, P., Bastin, S., Brut, A., Caccia, J. L., Campistron, B., Cautenet, S., Colette, A., Coll, I., Corsmeier, U., Cros, B., Dabas, A., Delbarre, H., Dufour, A., Durand, P., Guenard, V., Hasel, M., Kalthoff, N., Kottmeier, C., Lasry, F., Lemonsu, A., Lohou, F., Masson, V., Menut, L., Moppert, C., Peuch, V. H., Puygrenier, V., Reitebuch, O., and Vautard, R.: Regional transport and dilution during high-pollution episodes in southern France: Summary of findings from the Field Experiment to Constraint Models of Atmospheric Pollution and Emissions Transport (ESCOMPTE), J. Geophys. Res.-Atmos. 112, D13105, doi:10.1029/2006JD007494, 2007.
Evtyugina, M. G., Nunes, T., Pio, C., and Costa, C. S.: Photochemical pollution under sea breeze conditions, during summer, at the Portuguese West Coast, Atmos. Environ., 40, 6277–6293, 2006.
Farr, T. G., Rosen, P. A., Caro, E., Crippen, R., Duren, R., Hensley, S., Kobrick, M., Paller, M., Rodriguez, E., Roth, L., Seal, D., Shaffer, S., Shimada, J., Umland, J., Werner, M., Oskin, M., Burbank, D., and Alsdorf, D.: The shuttle radar topography mission, Rev. Geophys., 45, RG2004, doi:10.1029/2005RG000183, 2007.
Fisher, B., Joffre, S., Kukkonen, J., Piringer, M., Rotach, M. W., and Schatzmann, M.: Meteorology applied to Urban Air Pollution Problems, Final Report COST Action 715, Demetra Ltd. Publishers, Bulgaria, 2005.
Geleyn, J. F., Banciu, D., Bubnova, R., Ihasz, I., Ivanovici, V., LeMoigne, P., and Radnoti, G.: The International Project ALADIN: Summary of Events October 1992–October 1993. LAM Newsletter 23, 1992.
Grisogono, B., Kraljević, L., and Jeričević, A.: The low-level katabatic jet height versus Monin-Obukhov height, Q. J. Roy. Meteor. Soc., 133, 2133–2136, 2007.
Jeričević, A., Špoler Čanić K., and Vidič, S.: Prediction of stability and mixing height in the complex orography, Cro. Meteorol. J., 39, 3–14, 2004.
Jeričević, A., Kraljević, L., Vidič, S., and Tarrason, L.: Project description: High resolution environmental modelling and evaluation programme for Croatia (EMEP4HR), Geofizika, 24,

137–143, 2007, http://geofizika-journal.gfz.hr/abs24_2.htm#25.
Jeričević, A., Kraljević, L., Grisogono, B., and Fagerli, H.: Parametrization of vertical diffusion and the atmospheric boundary layer height determination in the EMEP model, in preparation, 2009.
Jimenez-Guerrero, P., Jorba, O., Baidasanoa, J. M., and Gasso, S.: The use of a modelling system as a tool for air quality management: Annual high-resolution simulations and evaluation, Sci. Total Environ., 390, 323–340, 2008.
Kain, J. S., Weiss, S. J., Levit, J. J., Baldwin, M. E., and Bright, D. R.: Examination of convection-allowing configurations of the WRF model for the prediction of severe convective weather: The SPC/NSSL Spring Program 2004, Weather Forecast., 21, 167–181, 2006.
Klaić, Z.: A Lagrangian model of long-range transport of sulphur with the diurnal variations of some model parameters, J. Appl. Meteorol., 35, 574–585, 1996.
Klaić, Z. B.: Assesment of wintertime atmospheric input of European sulfur to the eastern Adriatic, Nuovo Cimento, 26C, 1–6, 2003.
Klaić, Z. B. and Beširević, S.: Modelled sulphur depositions over Croatia, Meteorol. Atmos. Phys., 65, 133–138, 1998.
Klaić, Z. B., Nitis, T., Kos, I., and Moussiopoulos, N.: Modification of the local winds due to hypothetical urbanization of the Zagreb surroundings, Meteorol. Atmos. Phys., 79, 1–12, 2002.
Klaić, Z. B. and Nitis, T.: Application of mesoscale model (MEMO) to the Greater Zagreb Area during summertime anticyclonic weather conditions, Geofizika, 18–19, 31–43, 2001–2002.
Klaić, Z. B., Belušić, D., Grubišić, V., Gabela, L., and Ćoso, L.: Mesoscale airflow structure over the northern Croatian coast during MAP IOP 15 – a major bora event, Geofizika, 20, 23–61, 2003.
Levy, I., Dayan, U., and Mahrer, Y.: A five-year study of coastal recirculation and its effect on air pollutants over the East Mediterranean region, J. Geophys. Res.-Atmos., 113, D16121, doi:10.1029/2007JD009529, 2008.
Mahrt, L. and Vickers, D.: Extremely weak mixing in stable conditions, Bound.-Lay. Meteorol., 119, 19–39, 2006.
Kunz, R. and Moussiopoulos, N.: Simulation of the wind-field in Athens using refined boundary-conditions, Atmos. Environ., 29, 3575–3591, 1995.
Mahrt, L.: The influence of nonstationarity on the turbulent flux-gradient relationship for stable stratification, Bound.-Lay. Meteorol., 125, 245–264, 2007.

Michalakes, J., Dudhia, J., Gill, D., Henderson, T., Klemp, J., Skamarock, W., and Wang, W.: The Weather Research and Forecasting Model: software architecture and performance, in: 11th ECMWF Workshop on the use of High Performance Computing in Meteorology, edited by: Mozdzynski, G., Reading, UK, 2004.

Moussiopoulos, N.: The Eumac Zooming-Model, a tool for local-to-regional air-quality studies, Meteorol. Atmos. Phys., 57, 115–133, 1995.

Natale, P., Anfossi, D., and Cassardo, C.: Analysis of an anomalous case of high air pollution concentration in Turin after a foehn event, Int. J. Environ. Pollut., 11, 147–164, 1999.

Nitis, T., Kitsiou, D., Klaić, Z. B., Prtenjak, M. T., and Moussiopoulos, N.: The effects of basic flow and topography on the development of the sea breeze over a complex coastal environment, Q. J. Roy. Meteor. Soc., 131, 305–328, 2005.

Nitis, T., Tsegas, G., Korres, G., Douros, I., and Moussiopoulos, N.: Influence of sea surface temperature variation on basic mesoscale flows over coastal areas, in: Proceedings of the 10th international conference on "Environmental Science and Technology", Kos Island, Greece, 1037–1044, 2007.

Nitis, T., Klaić, Z. B., Kitsiou, D., and Moussiopoulos, N.: Meteorological simulations with use of satellite data for assessing Urban Heat Island under summertime anticyclonic conditions, Int. J. Environ. Pollut., in press, 2009.

O'Brien, J. J.: A note on the vertical structure of the Eddy Exchange Coefficient in the planetary boundary layer, J. Atmos. Sci., 27, 1213–1215, 1970.

Pohjola, M. A., Rantamaki, M., Kukkonen, J., Karppinen, A., and Berge, E.: Meteorological evaluation of a severe air pollution episode in Helsinki on 27–29 December 1995, Boreal Env. Res., 9, 75–87, 2004.

Prtenjak, M. T., Grisogono, B., and Nitis, T.: Shallow mesoscale flows at the north-eastern Adriatic coast, Q. J. Roy. Meteor. Soc., 132, 2191–2215, 2006.

Prtenjak, M. T. and Grisogono, B.: Sea/land breezes climatological characteristics along the northeastern Adriatic coast, Theor. Appl. Climatol., 90, 201–215, 2007.

Prtenjak, M. T., Pasarić, Z., Orlić, M., and Grisogono, B.: Rotation of sea/land breezes along the northeastern Adriatic coast, Ann. Geophys., 26, 1711–1724, 2008a, http://www.ann-geophys.net/26/1711/2008/.

Prtenjak, M. T., Nitis, T., and Klaić, Z. B.: Mesoscale modeling of atmospheric conditions during severe SO_2 episode in Rijeka, Croatia, in: Proceedings of the international conference on "Studying, Modeling and Sense Making of Planet Earth". Mytelene, University of Aegean,

1–8, 2008b.
Robinsohn, J., Mahrer, Y., and Wakshal, E.: The effects of mesoscale circulation on the dispersion of pollutants (SO_2) in the eastern Mediterranean, southern coastal-plain of Israel, Atmos. Environ., 26, 271–277, 1992.
Simpson, D., Fagerli, H., Jonson, J. E., Tsyro, S., Wind, P., and Tuovinen, J.-P.: Unified EMEP Model Description. EMEP Status Report 1/03, Part I. Oslo, Norway, 2003, http://www.emep.int/UniDoc/index.html.
Skamarock, W. C., Klemp, J. B., Dudhia, J., Gill, D. O., Barker, D. M., Wang, W., and Powers, J. G.: A description of the Advanced Research WRF Version 2, NCAR/TN-468+STR, NCAR TECHNICAL NOTE, 88 pp, January 2007, http://www.mmm.ucar.edu/wrf/users/docs/arw_v2.pdf.
Skamarock, W. C. and Klemp, J. B.: A time-split nonhydrostatic atmospheric model for weather research and forecasting applications, J. Comput. Phys., 227, 3465–3485, 2008.
Skouloudis, A. N., Kassomenos, P., and Nitis, T.: Science and policy challenges of atmospheric modelling in consideration of health effects, Int. J. Environ. Pollut., accepted, 2009.
Soler, M. R., Hinojosa, J., Bravo, M., Pino, D., and de Arellano, J. V. G.: Analyzing the basic features of different complex terrain flows by means of a Doppler Sodar and a numerical model: Some implications for air pollution problems, Meteorol. Atmos. Phys., 85, 141–154, 2004.
Soriano, C., Baldasano, J. M., Buttler, W. T., and Moore, K. R.: Circulatory patterns of air pollutants within the Barcelona air basin in a summertime situation: Lidar and numerical approaches, Bound.-Lay. Meteorol., 98, 33–55, 2001.
Steenkist, R.: Episodes of high SO_2 concentration in The Netherlands, Atmos. Environ., 22, 1475–1480, 1988.
Stull, R. B.: An Introduction to Boundary Layer Meteorology, Kluwer, Dordrecht, 1998.
Tayanc, M. and Bercin, A.: SO_2 modeling in Izmit Gulf, Turkey during the winter of 1997: 3 cases, Environ. Model. Assess., 12, 119–129, 2007.
Trenberth, K. E., Davis, C. A., and Fasullo, J.: Water and energy budgets of hurricanes: Case studies of Ivan and Katrina, J. Geophys. Res.-Atmos., 112, D23106, doi:10.1029/2006JD008303, 2007.
Vieno, M., Dore, A. J., Wind, P., Di Marco, C., Nemitz, E., Phillips, G., Tarrason, L., and Sutton, M. A.: Application of the EMEP Unified Model to the UK with a horizontal resolution of 5×5 km^2, in: Atmospheric Ammonia: Detecting emission changes and environmental im-

pacts, edited by: Sutton, M. A., Baker, S., and Reis, S., Springer, 464 pp., in press, 2009.
Vieno, M., Dore, A. J., Stevenson, D. S., Doherty, R., Heal, M., Reis, S., Hallsworth, S., Tarrason, L., Wind, P., Fowler, D., Simpson, D., and Sutton, M. A.: Modelling surface ozone during the 2003 heat wave in the UK, Croatian Meteorological Journal 43, The 12th International Conference on Harmonizaton within Atmospheric Dispersion Modelling for Regulatory Purposes, HARMO 12, edited by: Djuričić, V., Zagreb, Croatian Meteorological Society, 83–87, 2008.
Willmott, C. J.: Some comments on the evaluation of model performance, B. Am. Meteorol. Soc., 63, 1309–1313, 1982.

Table 1. Details of measuring sites in the north-eastern Adriatic used in the study (see also Fig. 1). In the table, a station type (ST) is given by the abbreviations: M, O, AQ and RS that mean the main meteorological station, ordinary meteorological station, air quality monitoring and radio-sounding station, respectively. Temporal resolution (T) of the ordinary meteorological station corresponds to the three following terms: 07:00 LT, 14:00 LT and 21:00 LT.

Site code	Site name	ST	T (h)	Lat	Long	a.s.l. (m)	Geographical specifications
1	Pula-airport	M	24	44.9°	13.9°	63	SW Istrian coast near tip of peninsula, 10 km from the NW coast
2	Učka	M	24	45.3°	14.2°	1372	at top of the mountain of Učka
3A	Rijeka	M	24	45.3°	14.5°	120	at the eastern side of the Rijeka Bay 1 km far from the coast
3B	Rijeka	AQ	24	45.3°	14.4°	20	at the coast at the eastern side of the Rijeka Bay
4	Rijeka-airport	M	8	45.2°	14.5°	85	2 km from the NW coast at the island of Krk
5	Senj	M	24	44.9°	14.9°	26	on the borderline between two mountains – V. Kapela and Velebit, 0.5 km from the coast
6	Pazin	O	3	45.2°	13.9°	291	in the very centre of Istrian peninsula, 30 km from the coast
7	Botonega	O	3	45.3°	13.9°	50	in the wind protected area near small river lake in the middle of Istria
8	Abrami	O	3	45.4°	13.9°	85	in the wind protected area in the middle of Istria
9	Crikvenica	O	3	45.2°	14.7°	2	in the coastal zone squeezed between the sea and the island of Krk
10	Ponikve	O	3	45.1°	14.6°	25	northward above town Krk near the SE coast
11	Krk	O	3	45.0°	14.6°	9	at the SE coast of the island of Krk
12	Udine	RS	4	46.0°	13.2°	94	In the hinterland in Italy

ACPD
9, 6283–6324, 2009

Table 2. Index of agreement values for the wind speed, wind direction and 2-m air temperature modelled by WRF model during period 2–5 February 2002. This statistic index reflects the degree to which measurements are accurately estimated by the model.

Site code	Site name	Wind speed	Wind dir	Temp
1	Pula-airport	0.7	0.9	0.5
2	Učka	0.5	0.9	–
3A	Rijeka	0.3	0.8	0.6
5	Senj	0.5	0.9	0.8

ACPD
9, 6283–6324, 2009

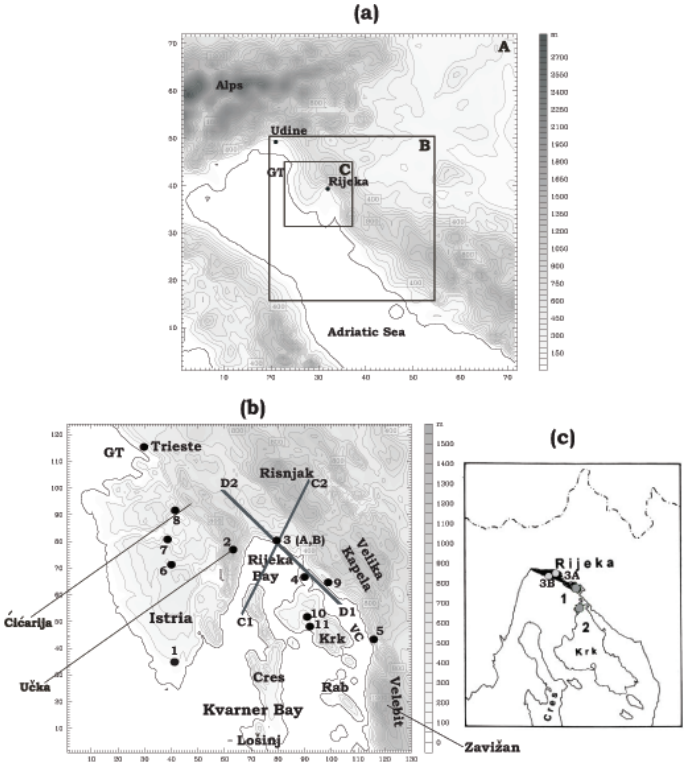

Fig. 1. Configuration of nested WRF grids over the study area on the north-eastern Adriatic coast. Frames indicate the coarse (A), medium (B) and the fine grid (C) WRF model domains, respectively. **(a)** Anaglyph for the fine-grid domain. Positions of routine measuring sites are shown by filled circles (see text for details). Lines C1C2 and D1D2 show bases of vertical cross-sections investigated in the Sect. 6. **(b)** Major industrial areas in the Greater Rijeka Area (GRA) are shown by circles filled in medium gray: 1 – industrial zone of Rijeka with, among others, an oil refinery and thermo-power plant, 2 – Petrochemical plant and the oil terminal (Omišalj, Krk island). The town of Rijeka is hatched in black and the position of the two measuring sites in Rijeka (3A and 3B) is presented by circles filled in light gray **(c)**.

ACPD
9, 6283–6324, 2009

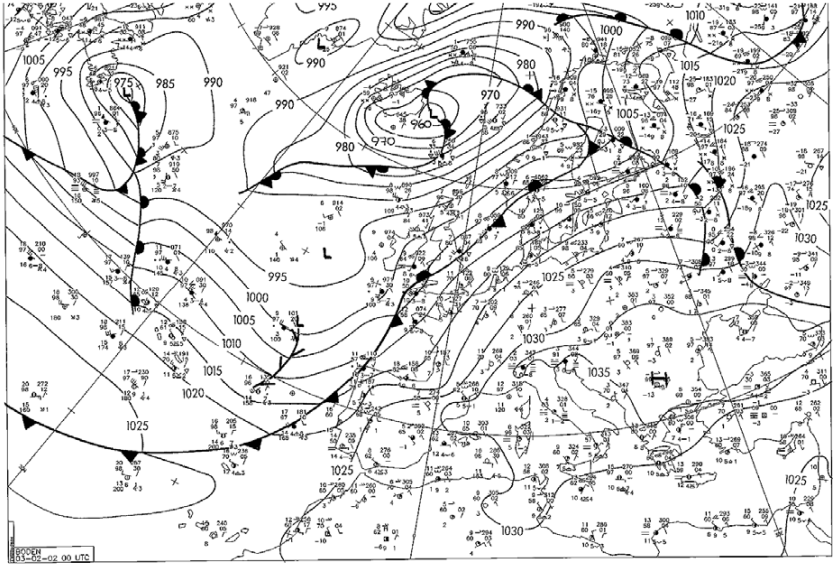

Fig. 2. Surface diagnostic charts for Europe at 00:00 UTC on 3 February 2002. (Source: European Meteorological Bulletin).

ACPD

9, 6283–6324, 2009

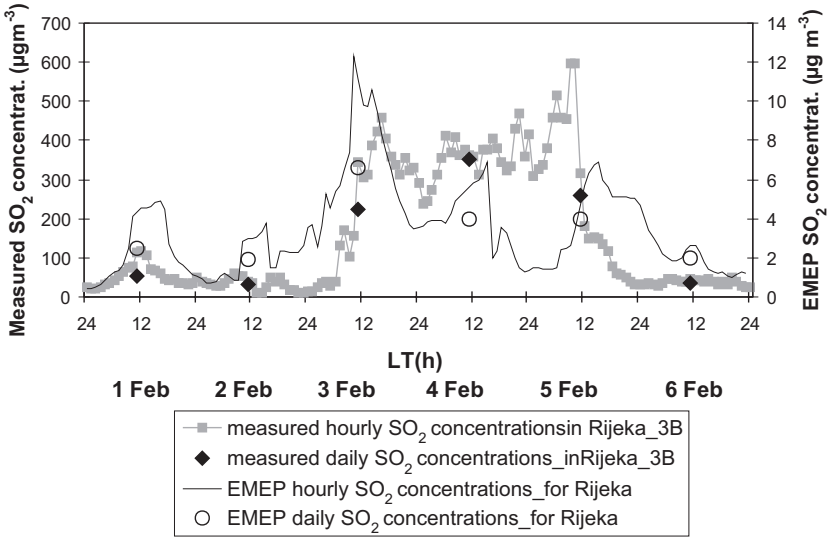

Fig. 3. The hourly (gray line with square) and daily mean (black rhomb) SO_2 concentrations measured at Rijeka (station 3B in Table and Fig. 1) (see y-axis on the left) as well as EMEP hourly (solid black line) and daily (circles) concentrations (see second y-axis on the right) from 1 to 6 February 2002. (Source for SO_2 measurements: Teaching Institute for Public Health, Rijeka.)

ACPD
9, 6283–6324, 2009

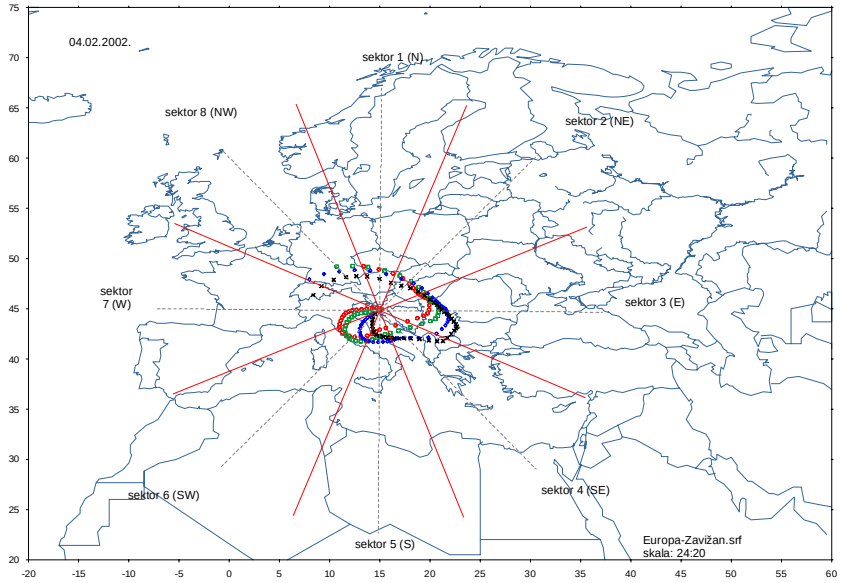

Fig. 4. 4-day backward 925 hPa trajectories arriving at Zavižan (see Fig. 1b) on 4 February 2002, at 00:00 UTC (black), 06:00 UTC (blue), 12:00 UTC (green) and 18:00 UTC (red). Parcel positions are given for every second hour.

ACPD
9, 6283–6324, 2009

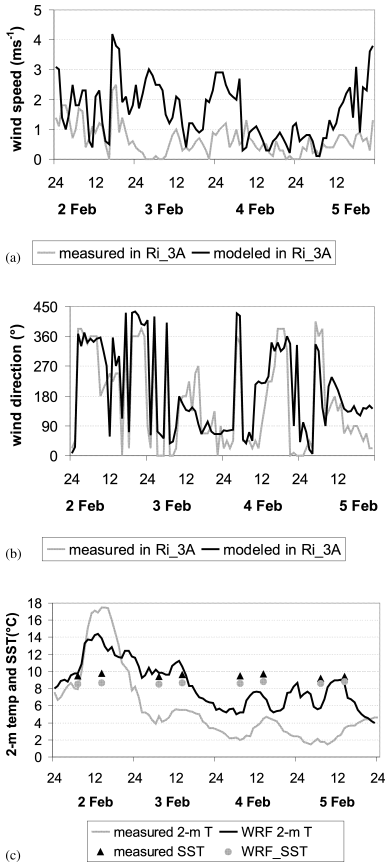

Fig. 5. The wind speed **(a)**, wind direction **(b)**, air temperature at 2 m height **(c)** from measurements (gray) and WRF model simulations (black) in 3A (Rijeka) station from 2 February 2002, till 5 February 2002. At **(c)** panel black triangles and gray circles correspond to the measured and WRF SST, respectively.

ACPD
9, 6283–6324, 2009

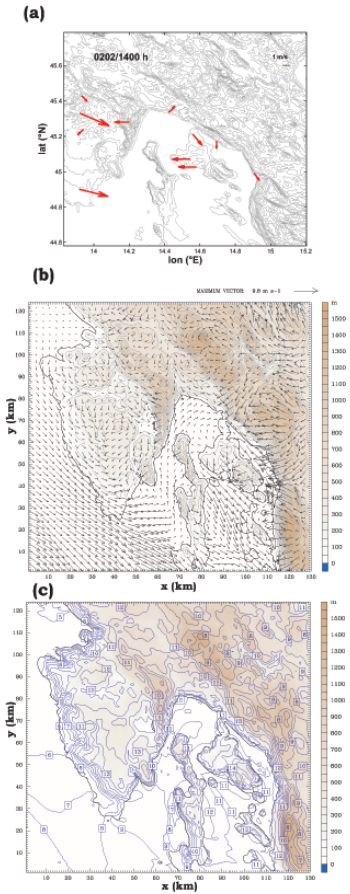

Fig. 6. The 10-m wind ($m\,s^{-1}$) from main and ordinary meteorological stations in Table **(a)**; modelled WRF wind field **(b)**; and WRF surface air temperature in $^{\circ}C$ **(c)** for 2 February 2002 at 14:00 LT.

ACPD
9, 6283–6324, 2009

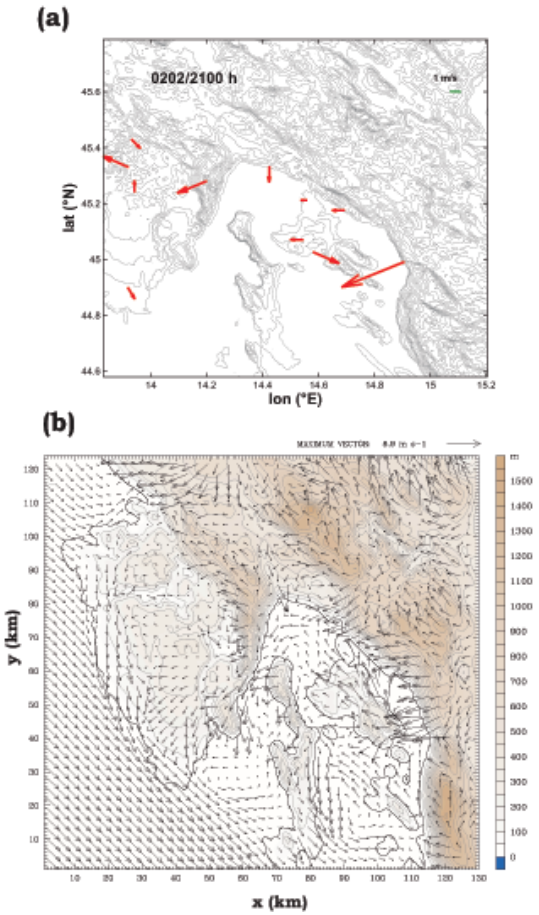

Fig. 7. The 10-m wind from main and ordinary meteorological stations **(a)** and WRF model simulations of wind **(b)** on 2 February 2002 at 21:00 LT.

ACPD
9, 6283–6324, 2009

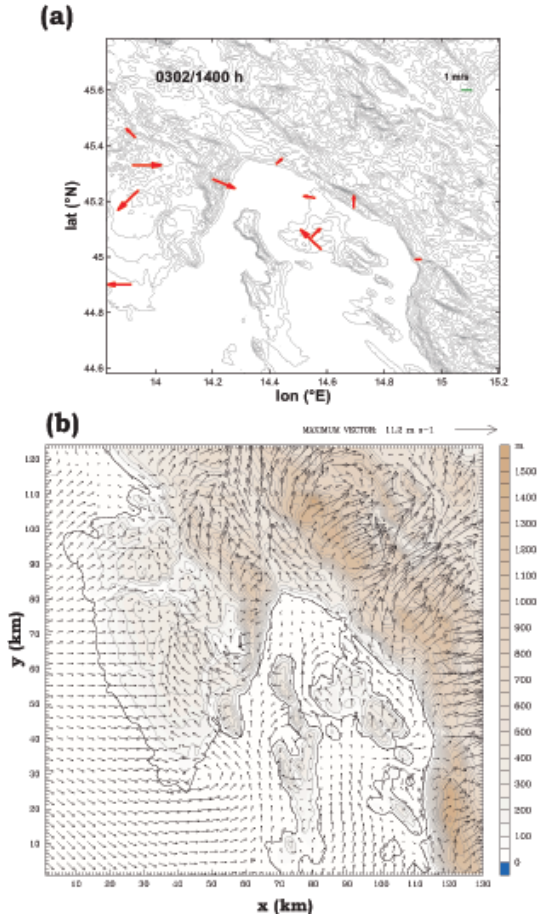

Fig. 8. Same as Fig. 6 except on 3 February 2002 at 14:00 LT.

ACPD
9, 6283–6324, 2009

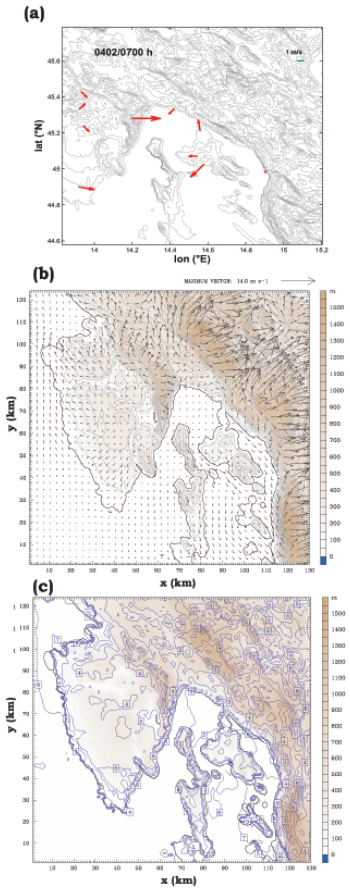

Fig. 9. The 10-m wind ($m\,s^{-1}$) from main and ordinary meteorological stations **(a)** and WRF model simulations of wind **(b)** and WRF surface air temperature in °C **(c)** on 4 February 2002 at 07:00 LT.

ACPD
9, 6283–6324, 2009

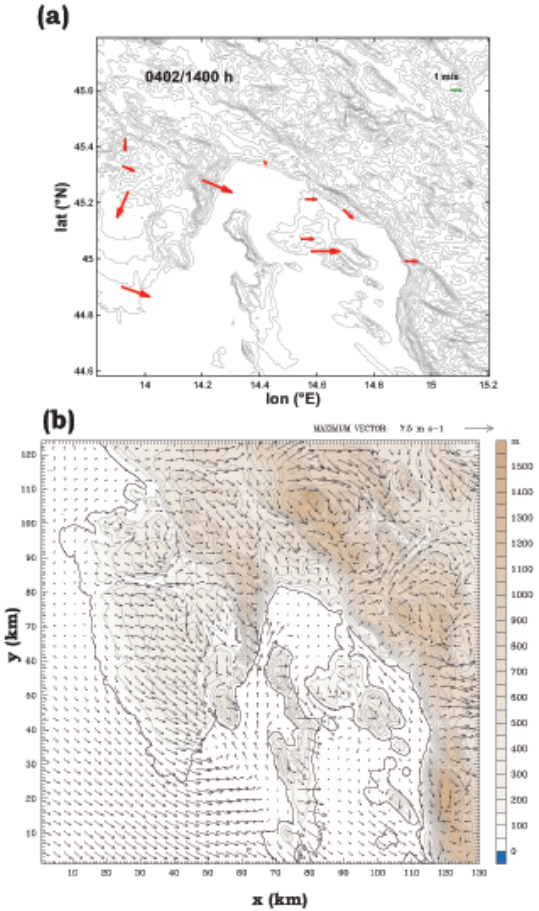

Fig. 10. Same as Fig. 6 except on 4 February 2002 at 14:00 LT.

ACPD
9, 6283–6324, 2009

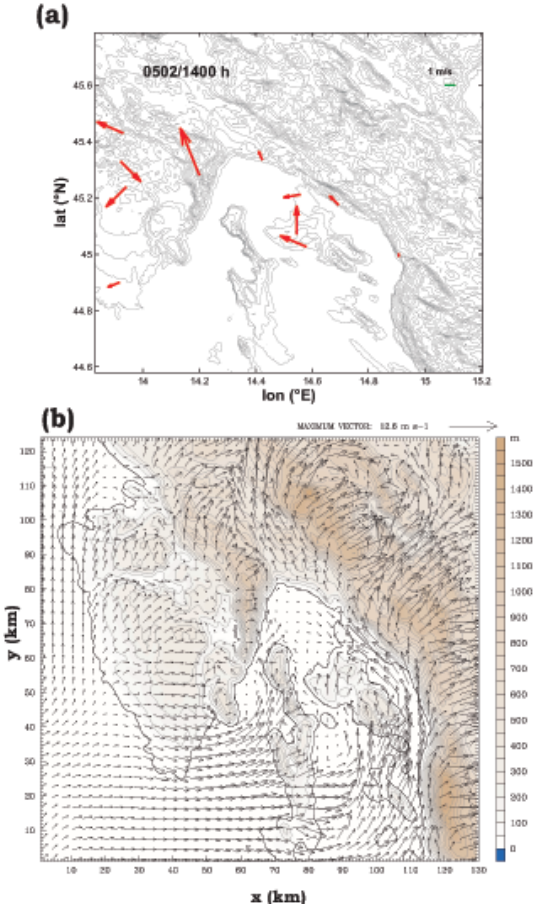

Fig. 11. Same as Fig. 6 except on 5 February 2002 at 14:00 LT.

ACPD
9, 6283–6324, 2009

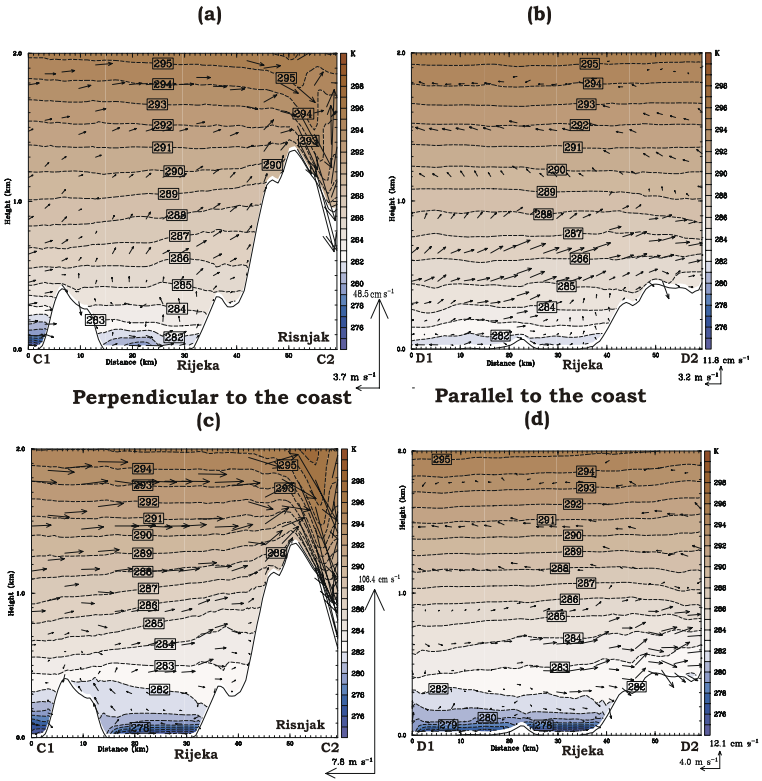

Fig. 12. Vertical cross-sections of the WRF modelled wind ($m\,s^{-1}$) and potential temperature (K) above Rijeka on 3 February 2002 at 09:00 LT (**a** and **b**) and 18:00 LT (**c** and **d**). Left and right panels correspond to the cross-sections perpendicular (C1C2) and parallel (D1D2) to the coastline. Bases of the cross-sections are shown in Fig. 1b.

ACPD
9, 6283–6324, 2009

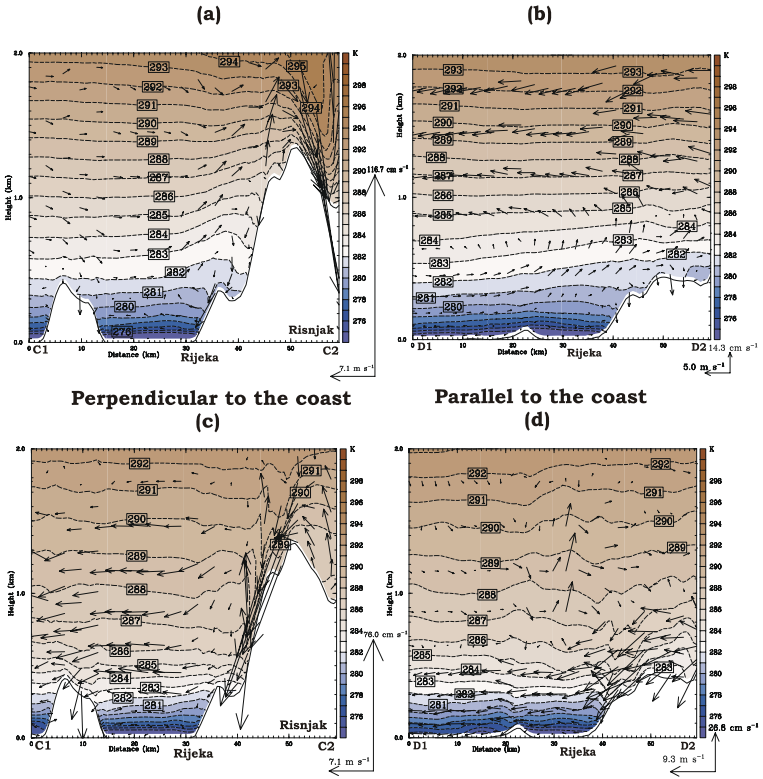

Fig. 13. Same as Fig. 12 except on 4 February 2002 at 08:00 LT (**a** and **b**) and 19:00 LT (**c** and **d**).

ACPD
9, 6283–6324, 2009

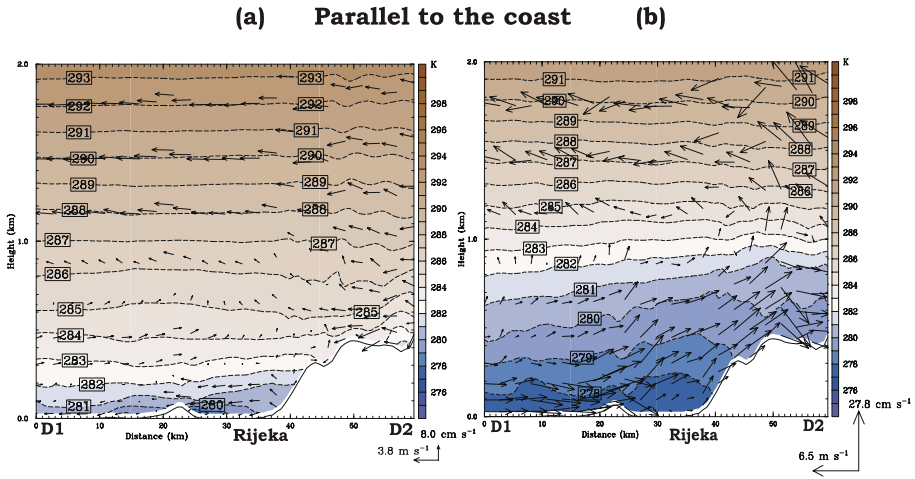

Fig. 14. Vertical cross-sections of the WRF modelled wind ($m\,s^{-1}$) and potential temperature (K) above Rijeka on 5 February 2002 at 08:00 LT **(a)** and 19:00 LT **(b)** along parallel cross-section (A1) to the coastline. Base of the D1D2 cross-section is shown in Fig. 1b.

ACPD
9, 6283–6324, 2009

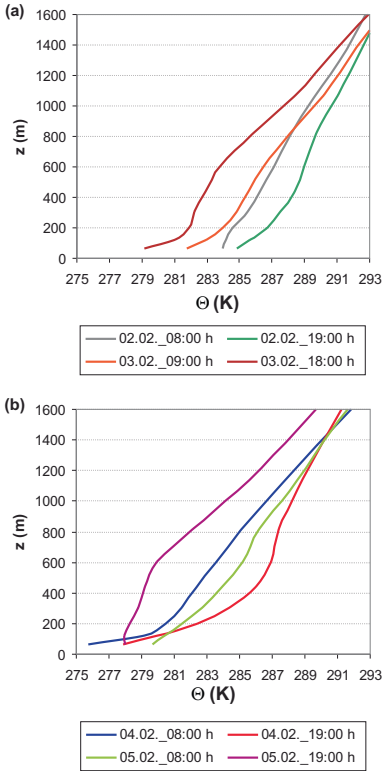

Fig. 15. Modelled WRF vertical profiles of potential temperature (K) from 2 to 5 February 2002 above Rijeka. Times correspond to the times of cross-sections shown in Figs. 13–15.

ACPD
9, 6283–6324, 2009

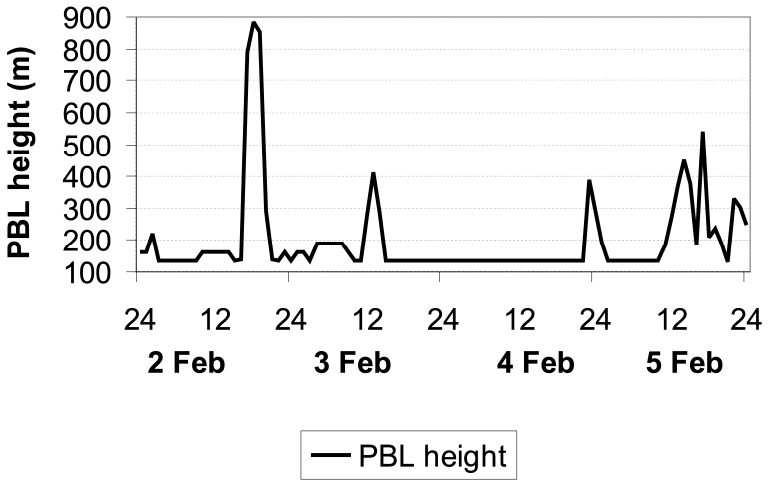

Fig. 16. The daily course of the modelled WRF planetary boundary layer height (m) obtained for Rijeka from 2 to 5 February 2002.